EUROPEAN ENDODONTIC JOURNAL

ORIGINAL ARTICLE

Influence of Different Glide Path Techniques on Microcrack Formation after Two Different Root Canal Preparation Treatments: Micro Computed Tomography Analysis

Shang Fuad JAMAL, Ranjdar Mahmood TALABANI

Department of Conservative, College of Dentistry, University of Sulaimani, Sulaimani, Iraq

ABSTRACT

Objective: This study aimed to evaluate the effect of WaveOne Glider (WOGG) with Waveone Gold (WOG) primary reciprocation systems on root dentine microcrack formation and to know the effect of TruNatomy Glider (TRNG) with TruNatomy (TRN) prime rotary systems on root dentine microcrack formation.

Methods: In this study, 40 extracted mandibular first molar roots were selected and divided randomly into four groups (n=10). Group MWOG: a manual glide path was performed + WOG primary. Group MTRN: manual glide path performed+TRN prime. Additionally, group WOGG: glide path preparation with WOGG+WOG primary. Finally, for group TRNG, the glide path preparation was performed with TRNG+TRN prime. Micro-CT was used for pre and post-instrumentation image analysis. Statistical analysis was performed using the Kruskal-Wallis test ($p<0.05$) with Two-way ANOVA.

Results: The Kruskal-Wallis test showed no significant differences among all groups in all thirds for pre and post-instrumentation regarding the crack formation. The Two-way ANOVA showed no significant difference or interaction between the ways of glide path preparation, whether manual or reciprocal WOGG, or between the rotary TRNG and the motion used in root canal preparation (rotary TRN or reciprocal WOG) regarding the crack formation and propagation.

Conclusion: Microcrack formation and propagation occurred independently of using different glide path techniques (manual, rotary, or reciprocal).

Keywords: Glide path, micro-computed tomography, microcrack, TruNatomy Glider, TruNatomy, WaveOne Glider

Please cite this article as: Jamal SF, Talabani RM. Influence of Different Glide Path Techniques on Microcrack Formation after Two Different Root Canal Preparation Treatments: Micro Computed Tomography Analysis. Eur Endod J 2024; 9: 124-32

Address for correspondence:
Shang Fuad Jamal
Department of Conservative, University of Sulaimani College of Dentistry, Sulaimani, Iraq
E-mail: shang9054@gmail.com

Received September 08, 2023, Revised October 08, 2023, Accepted October 25, 2023

Published online: March 05, 2024
DOI 10.14744/eej.2023.20982

HIGHLIGHTS

- Dentinal microcracks are a clinical problem to treat and may propagate to vertical root fractures, leading to tooth extraction.
- Creating a glide path before canal preparation may reduce the incidence of microcrack formation. Engine-driven pathfinding files provide better results in reducing microcrack formation than manually created glide paths.

INTRODUCTION

Primarily, root canal shaping in endodontic treatment is confined within the root canal space and performed using different kinematics instruments for efficient dentine disinfection (1). This instrumentation procedure may be linked to inducing or propagating dentinal microcracks by generating stress (2). Dentinal microcrack is a severe clinical problem that reduces tooth resistance and can lead to vertical root fracture, especially after applying occlusal forces (3). Dentinal microcracks routinely occur after instrumentation and can be attributed to friction between the file and canal wall (4).

Nowadays, advanced technology in the field of imaging is leading to more understanding of dentinal microcracks. The introduction of micro-computed tomography as a highly accurate and nondestructive method has allowed accurate evaluation of many tooth sections to detect microcrack locations and enables correlations between the dentinal defects and other outcomes, such as the percentage of the canal surface touched by the instrument or even the location of stress concentration areas (5).

In past years, many NiTi rotary files with different kinematics (rotary and reciprocation) have been introduced for root canal preparation, with advantages such as high torsional stiffness and flexibility (6, 7). TruNatomy (TRN) rotary files (DentsplySirona, Ballaigues, Switzerland) are recently introduced endodontic files manufactured from a post-manufacture heat-treated NiTi alloy that has a parallelogram off-centred cross-sectional design with rotation motion (8).

On the other hand, the reciprocating files have repetitive up-and-down or back-and-forth motion to avoid the screw-in effect that happens with some continuous rotary instruments caused by rotational motion and may reduce the risk of file fracture (9). The WaveOne Gold (WOG) (DentsplySirona) systems have reduced the cyclic fatigue compared to NiTi rotary instruments caused by rotational motion and may reduce the risk of file fracture (9). The WOG reciprocating instruments are a modified version of WaveOne, manufactured from a thermally processed gold wire in a parallelogram-shaped cross-section design with two 85° cutting edges (10).

A glide path is a regular opening that extends from the orifice of the root canal to the apical foramen. Creating a glide path is important for root anatomy evaluation to provide an unobstructed path that thus reduces the torsional stress on the dentine wall, thereby reducing the incidence of root crack formation (11, 12). Many rotary path-finding systems are also available, including the TruNatomy Glider (TRNG), which has a centred and parallelogram-shaped cross-section made from post-manufactured heat-treated NiTi alloy (11). In contrast, the WaveOne Gold Glider (WOGG) is a single-use reciprocal file constructed from gold wire that has undergone thermo-mechanical treatment and has a parallelogram-shaped cross-section (13).

Many studies have investigated the incidence of dentinal microcracks associated with different glide path instruments. However, no research deals with the effect of glide paths on creating dentinal microcracks during root canal preparation using WOGG+WOG primary and TRNG+TRN prime.

Furthermore, the current study is the first to examine two distinct kinematics, rotation (TRNG+TRN prime) and reciprocation (WOGG+WOG primary), for the preparation of the root canal and the glide path, as well as their impacts on crack initiation and propagation.

This study aimed to assess the effect of different glide path techniques in dentinal microcrack formation after two different kinematic root canal preparations. The null hypothesis was tested: no difference was identified between different kinematic glide paths and root canal files in their effect on dentinal microcrack formation and propagation.

MATERIALS AND METHODS

In this *in-vitro* study, the sample size was determined using GPower v 3.1 (Universität Düsseldorf, Düsseldorf, Germany), indicating that each group's sample size should be at least 10. To conduct this study, 40 permanent mandibular first molars (MFMs) with 3 root canals (mesio-lingual, mesio-buccal, and distal) were selected from a group of teeth extracted for purposes unrelated to this study.

A CBCT machine CS9600 (Carestream Dental, Atlanta, US) was used to image all samples to determine whether to include or exclude the selected teeth. A putty impression material (Durosill, Allershausen, Germany) was used to form a mould to hold the samples during CBCT scanning. The images were viewed using CS 3D imaging software (v 3.10.21), the voxel size for the images was (150 μm×150 μm×150 μm), and the radiation dose (496 mGy.cm^2) with exposure was (120 KV 4 mA 15 s).

The selected teeth should have mesial roots with Vertucci type IV canal configuration, roots with closed apex, be free of root caries, and have root curvatures between 25–35°, according to the Schneider method (Fig. 1) (14). All root canals were determined by setting CBCT imaging to be from (18–21 mm) in length.

Any teeth with root curvature less than 25° or more than 35°, C-shaped canal, previous endodontic treatment, roots with open apex, presence of pulp stone, or calcified canal were excluded from this study. The selected samples were disinfected with 5.2% NaOCl (TehnoDent, Severnyi, Russia) and kept in distilled water until use (15).

The samples (n=40) were randomly and equally divided into four groups. In group MWOG, a manual glide path was performed, and root canal shaping was done with WOG primary. In group MTRN, the manual glide path was performed, and the TRN prime was used for canal shaping. In group WOGG, the reciprocal WOGG was used for glide path preparation, and WOG primary was used for canal shaping. Lastly, in group TRNG, a rotation glide path was performed by TRNG and the TRN prime was used for root canal shaping.

- Group MWOG (n=10): the canal patency was checked, and a manual glide path was created with 10# K-file until it reached 15# (MANI, Utsunomiya, Japan). Then, the WOG primary (25/v0.07) was used for canal shaping. The speed and torque (300 rpm/3 Ncm) were selected using the pre-programmed WOG setting on the X-Smart IQ endo motor. After shaping 3 mm, the file was removed and cleaned with 2 mL saline (LINCOLN, Sola, India) and sterile gauze. After three passes, the entire length was reached.
- Group MTRN (n=10): the glide path was created with #10 K-File to size 15#. The canal shaping was performed using TRN prime (26/v0.04) with (500 rpm/1.5 Ncm), which was selected using the pre-programmed X-Smart IQ endo motor. After shaping 3 mm, the file was cleaned with 2 mL saline and sterile gauze. After three passes, the entire working length was reached.
- Group WOGG (n=10): The reciprocal WOGG (15/0.02–0.06) was used for performing the glide path, with the speed

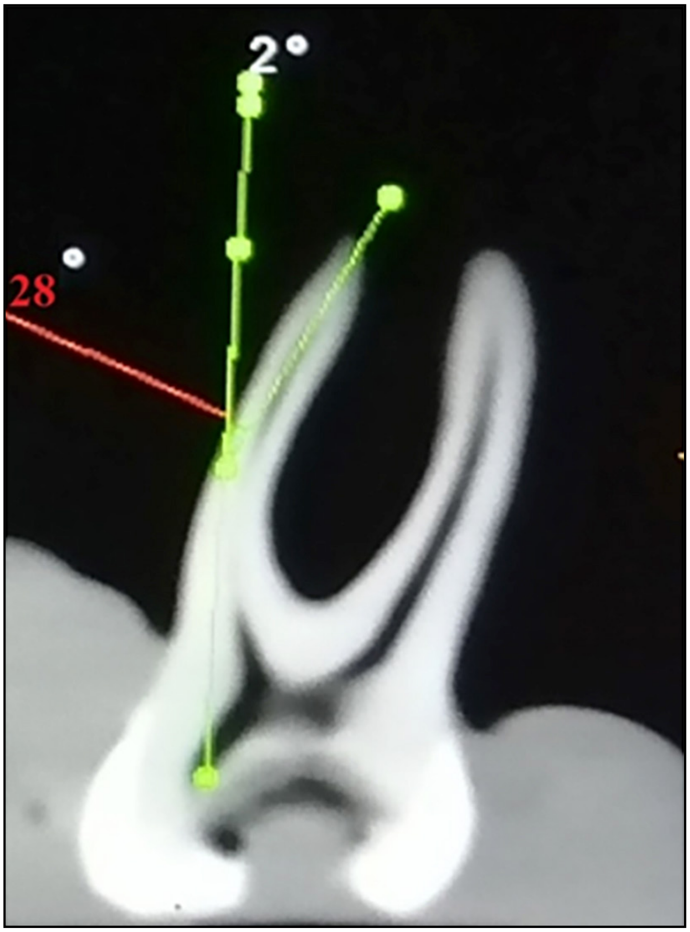

Figure 1. CBCT image shows root canal curvature

CBCT: Cone-beam computed tomography

and torque selected using the pre-programmed X-Smart IQ endo motor. When the glide path had been created, the canal shaping was finished using WOG primary to establish the entire working length.

- Group TRNG (n=10): The TRNG (17/v0.02) performed the glide path before canal instrumentation. The speed and torque were selected using the pre-programmed X-Smart IQ endo motor (500 rpm/1.5 Ncm). When the glide path had been created, the canals were shaped by TRN prime to full working length (WL).

Irrigation for all canals was done with 2 mL of 5.2% NaOCl between each instrumentation 2 mm shorter from the WL, using 30 gauge double-side vented endodontic irrigation needles (Pacotech, Texas, USA). The irrigation was finished using 5 mL of 17% EDTA (PrevestDenPro, Jammu, India) for 2 minutes, then with 5 mL of distilled water (16).

Micro-Computed Tomography Evaluation

In this study, for pre and post-instrumentation scanning, a micro-CT scanner LOTUS-*in Vivo* was used (LOTUS *inVivo*, Behin Negareh, Tehran, Iran), which has a cone beam micro-focus X-ray source and a flat panel detector. The X-ray tube voltage was set to 80 kV, its current was set to 80 µA, and the frame exposure time was set to 2 seconds by 3.5×magnification. The total scan duration was 49 minutes. Slice thicknesses of reconstructed images were set to 20 µm, selected in the coronal, middle, and apical thirds. The whole protocol settings process was controlled by LOTUS-*in Vivo*-ACQ software. The acquired 3D data were reconstructed using LOTUS *inVivo*-REC by a standard Feldkamp, Davis, Kress (FDK) algorithm.

All cross-sectional images (n=430) for all roots of MFMs at all thirds (coronal, middle, and apical) and planes (sagittal, coronal, and axial) were examined for the presence of cracks. The number of dentinal microcracks in each slice at all thirds was counted after postoperative slices were examined. The existence or absence of such defects was then confirmed using the identical scan slices from the preoperative images. All images were analysed to determine the percentage and number of new and propagated cracks. Two observers examined all images at the same time within one week. All types of defects observed were scored according to a previous study (16) as follows:

- Score 1: The craze line extends from the root's surface into the root dentine without reaching the canal wall.
- Score 2: Incomplete crack extends from root dentine without reaching the surface.
- Score 3: Complete crack extends from the root dentine to the canal wall.

Statistical Analysis

Data were entered into the Statistical Package for Social Sciences (SPSS, version 26, Chicago, IL, USA), which was then used to analyse the data. The Kruskal-Wallis test was utilised to compare the mean ranks of the teeth microcracks of the four study groups. Two-way Analysis of Variance (ANOVA) was used, where the dependent variable was the tooth microcrack score, and the independent variables were the glide path preparation methods and the canal preparation methods. Statistical significance was set at ($p<0.05$).

RESULTS

The inter-examiner agreement was calculated using weighted kappa statistics. The kappa statistics used to test inter-evaluator reliability showed that the reliability was 0.95, indicating a good inter-observer reliability.

Two-way ANOVA was used to study the effect of the kinematic of glide path preparation, canal shaping, and the interaction between them.

After the root canal preparation, no significant differences regarding microcrack formation (new and propagated) were detected between the different kinematics of glide path preparation ($p=0.773$) and the different kinematics of root canal preparation ($p=0.229$), as presented in Table 1, for the distal root at coronal third. The same finding emerged for the middle third, where $p=0.198$ was obtained for the glide path and $p=0.873$ for canal preparation. Also, for the apical third, the glide path result was $p=0.674$, and for canal preparation, it was $p=0.576$.

The same pattern can be observed in Table 2 and Table 3, where no significant differences were detected between the methods of glide path preparation and root canal preparation in terms of microcrack formation.

TABLE 1. Association of glide path and canal preparation methods with microcrack formation in distal roots

Roots/portions	Methods	n	Mean (microcrack)	SD	p*
Post-distal coronal	Glidepath preparation				0.773
	Manual	20	1.25	1.25	
	Reciprocal WOGG	10	1.00	1.25	
	Rotary TRNG	10	1.20	1.40	
	Root canal preparation				0.229
	WOG primary	20	0.95	1.05	
	TRN prime	20	1.40	1.43	
Post-distal middle	Glide path preparation				0.198
	Manual	20	1.65	1.35	
	Reciprocal WOGG	10	0.60	1.26	
	Rotary TRNG	10	1.30	1.49	
	Root canal preparation				0.873
	WOG primary	20	1.15	1.35	
	TRN prime	20	1.45	1.47	
Post-distal apical	Glidepath preparation				0.674
	Manual	20	0.30	0.57	
	Reciprocal WOGG	10	0.30	0.95	
	Rotary TRNG	10	0.50	0.97	
	Canal preparation				0.576
	WOG primary	20	0.35	0.81	
	TRN prime	20	0.35	0.75	

*: By Two-way ANOVA. n: Number, SD: Standard deviation, WOGG: Waveone Gold Glider, TRNG: TruNatomy Glider, WOG: Waveone Gold, TRN: TruNatomy, ANOVA: Analysis of Variance

TABLE 2. Association of glide path and root canal preparation methods with microcrack formation in the mesiobuccal roots

Roots/Portions	Methods	n	Mean (microcrack)	SD	p*
Post-mesiobuccal coronal	Glidepath preparation				0.185
	Manual	20	1.10	1.25	
	Reciprocal WOGG	10	0.40	0.97	
	Rotary TRNG	10	0.60	0.97	
	Root canal preparation				0.433
	WOG primary	20	0.85	1.09	
	TRN prime	20	0.75	1.21	
Post-mesiobuccal middle	Glidepath preparation				0.386
	Manual	20	1.15	1.42	
	Reciprocal WOGG	10	0.70	1.25	
	Rotary TRNG	10	0.50	0.97	
	Root canal preparation				0.392
	WOG primary	20	1.05	1.36	
	TRN prime	20	0.70	1.22	
Post-mesiobuccal apical	Glide path preparation				0.814
	Manual	20	0.20	0.62	
	Reciprocal WOGG	10	0.60	1.26	
	Rotary TRNG	10	0.10	0.32	
	Canal preparation				0.257
	WOG primary	20	0.50	1.05	
	TRN prime	20	0.05	0.22	

*: By Two-way ANOVA

For group MWOG and MTRN, where manual glide path was performed, as revealed in Figure 2, the group MTRN showed the best results on reducing crack formation at the coronal third (4.08%), followed by the middle third (10.20%). In contrast, the group MWOG showed more new cracks post-operatively at the middle third (20.41%), followed by the coronal third (12.24%).

For the groups WOGG and TRNG, where kinematics glide path was performed, as revealed in Figure 2, in group TRNG, where rotary glide path with TRNG was performed with TRN prime for canal shaping, the number and percentage of crack formation were lowest at the coronal third (8.16%), while in group WOGG the lowest percentage of newly formed cracks was in the apical third (0.00%), followed by the middle third (2.04%).

TABLE 3. Association of glide path and root canal preparation methods with microcrack formation in the mesiolingual roots

Roots/ Portions	Methods	n	Mean (microcrack)	SD	p*
Post-mesiolingual coronal	Glide-path preparation				0.552
	Manual	20	0.85	1.18	
	Reciprocal WOGG	10	0.50	1.08	
	Rotary TRNG	10	1.00	1.25	
	Root canal preparation				0.575
	WOG primary	20	0.75	1.12	
	TRN prime	20	0.85	1.23	
Post-mesiolingual middle	Glidepath preparation				0.361
	Manual	20	1.20	1.24	
	Reciprocal WOGG	10	0.70	1.16	
	Rotary TRNG	10	1.10	1.45	
	Root canal preparation				0.299
	WOG primary	20	1.10	1.29	
	TRN prime	20	1.00	1.26	
Post-mesiolingual apical	Glidepath preparation				0.495
	Manual	20	0.10	0.45	
	Reciprocal WOGG	10	0.20	0.63	
	Rotary TRNG	10	0.30	0.67	
	Root canal preparation				0.430
	WOG primary	20	0.20	0.62	
	TRN prime	20	0.15	0.49	

*: By Two way ANOVA

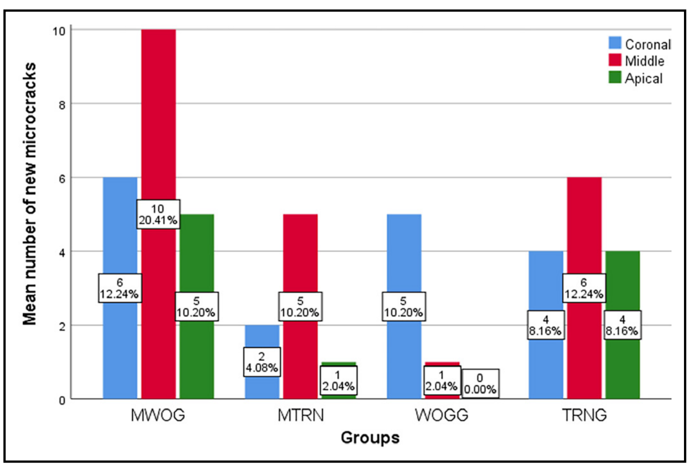

Figure 2. The total (combining at all levels) percentage and number of new microcracks formed after root canal preparation of study groups

MWOG: Manual glidepath+WOG primary, MTRN: Manual glidepath+TRN prime, WOGG: Waveone Gold Glider+WOG primary, TRNG: TruNatomy Glider+TRN prime

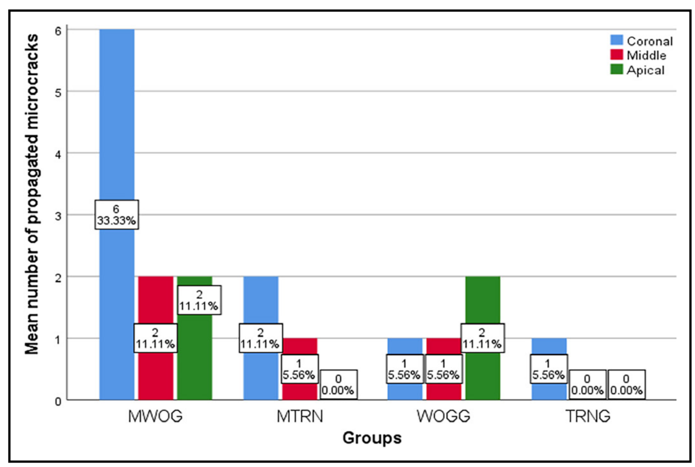

Figure 3. The total (combining all levels) percentage and number of post-instrumentation propagated microcracks after root canal preparation of study groups

Regarding crack propagation, in group MWOG, the propagated cracks increased, and the most were seen at the coronal third (33.33%), followed by the middle and coronal thirds (11.11%).

The MTRN showed better results in reducing crack propagation, especially in the apical third (0.00%), followed by the middle (5.56%) and coronal thirds (11.11%), as shown in Figure 3.

On the other hand, in group TRNG, the propagated cracks were reduced in all thirds (apical (0.00%), middle (0.00%), and coronal (5.56%)) when compared to group WOGG, in which the propagation occurred mostly at the apical third (11.11%), followed by the coronal and middle thirds (5.58%), as shown in (Fig. 3). Figures 4 to 7 are representative micro-CT images that show microcracks in all groups at all thirds and all roots before and after root canal preparation.

DISCUSSION

As indicated by the results of the present study, microcracks occurred in all groups regardless of the glide path preparation techniques. Therefore, the null hypothesis of the present study has been accepted. This study showed that the manual glide path with WOG for root canal shaping formed the highest number of microcracks. Meanwhile, the rotary glide path with TRNG and TRN prime for root canal shaping showed less effect on microcrack formation. Additionally, dentinal defects are low in the apical third, especially in the

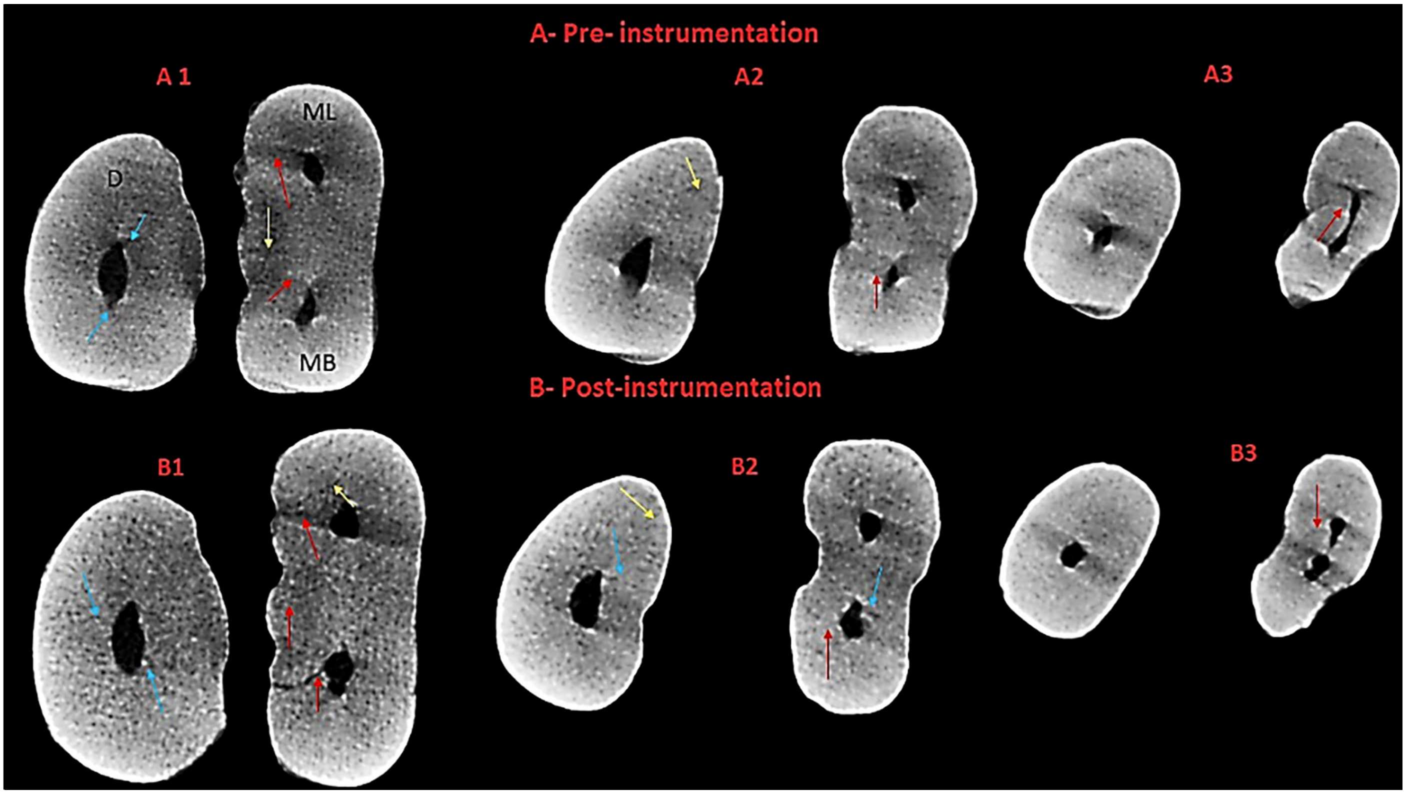

Figure 4. A: Micro-CT images for group MWOG pre-instrumentation showing microcracks as indicated by arrows (red: complete crack, blue: incomplete crack, yellow: craze line) at all levels: coronal (A1), middle (A2), and apical (A3). B: Micro-CT images post-instrumentation showing microcracks as indicated by arrows (red: complete crack, blue: incomplete crack, yellow: craze line) at all levels: coronal (B1), middle (B2), and apical (B3)

CT: Computed tomography

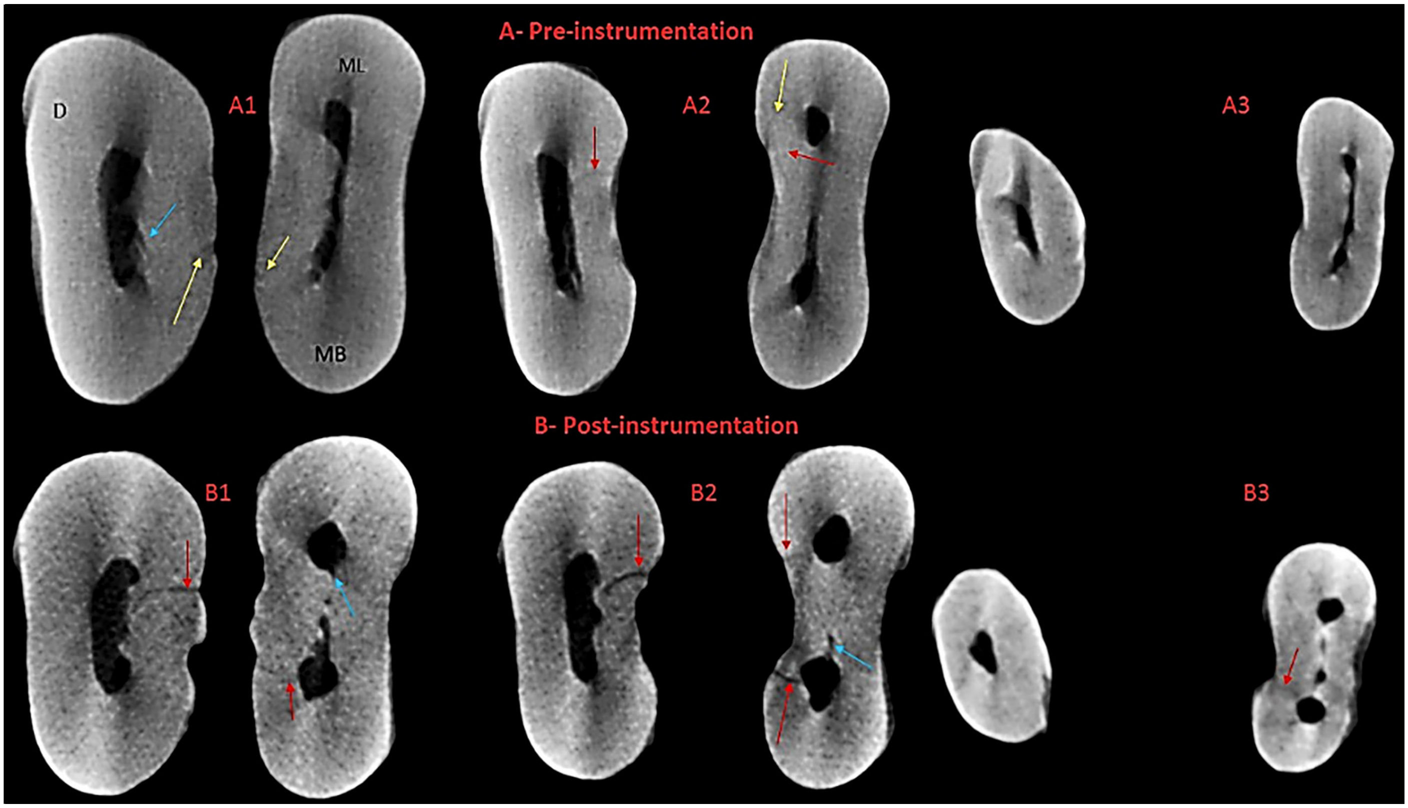

Figure 5. A: Micro-CT images for group MTRN pre-instrumentation showing microcracks at all levels: coronal (A1), middle (A2), apical (A3) as indicated by arrows (red: complete crack, blue: incomplete crack, yellow: craze line). B: Micro-CT images post-instrumentation showing microcracks at all levels: coronal (B1), middle (B2), apical (B3) as indicated by arrows (red: complete crack, blue: incomplete crack, yellow: craze line)

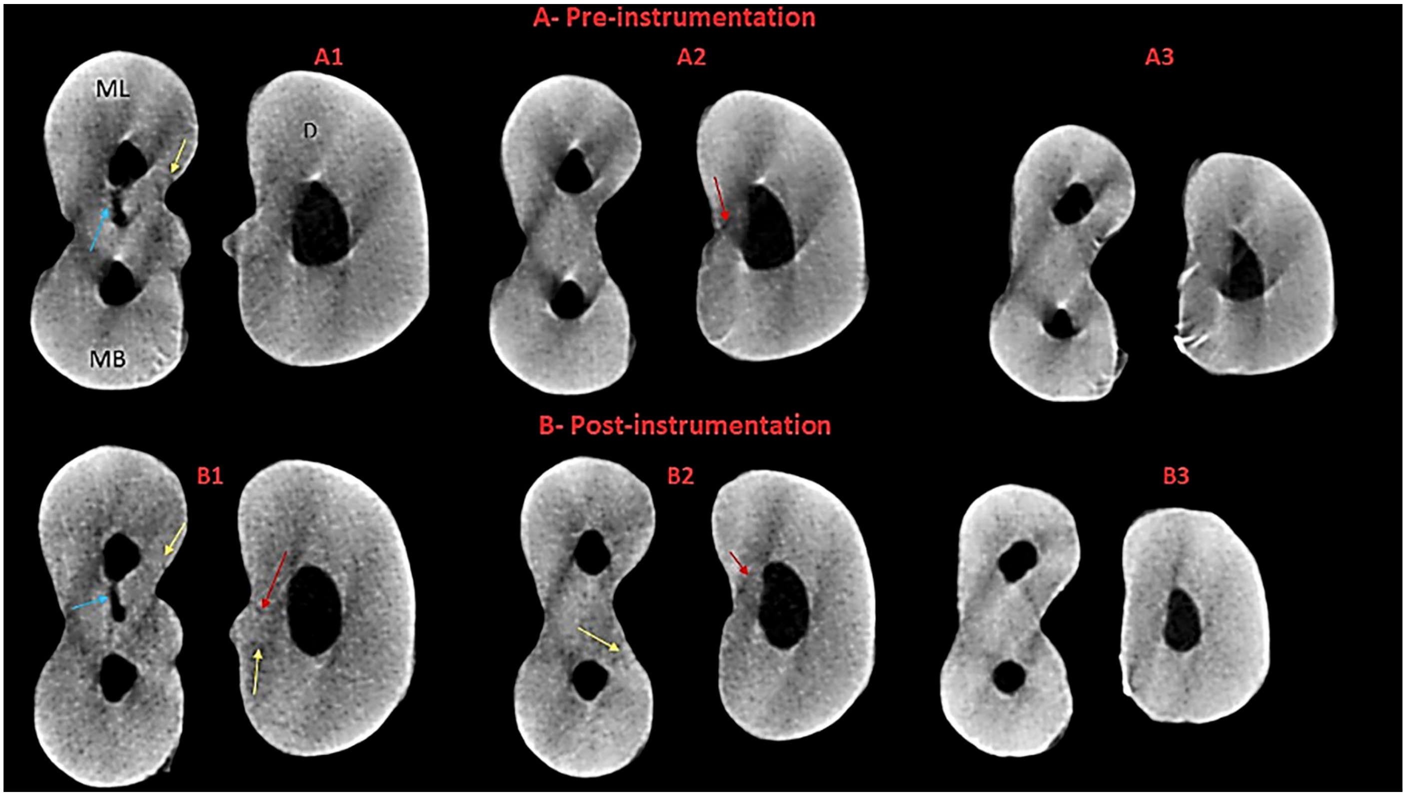

Figure 6. A: Micro-CT images for group WOGG pre-instrumentation showing microcracks at all levels: coronal (A1), middle (A2), apical (A3) as indicated by arrows (red: complete crack, blue: incomplete crack, yellow: craze line). B: Micro-CT images post-instrumentation showing microcracks at all levels: coronal (B1), middle (B2), apical (B3) as indicated by arrows (red: complete crack, blue: incomplete crack, yellow: craze line)

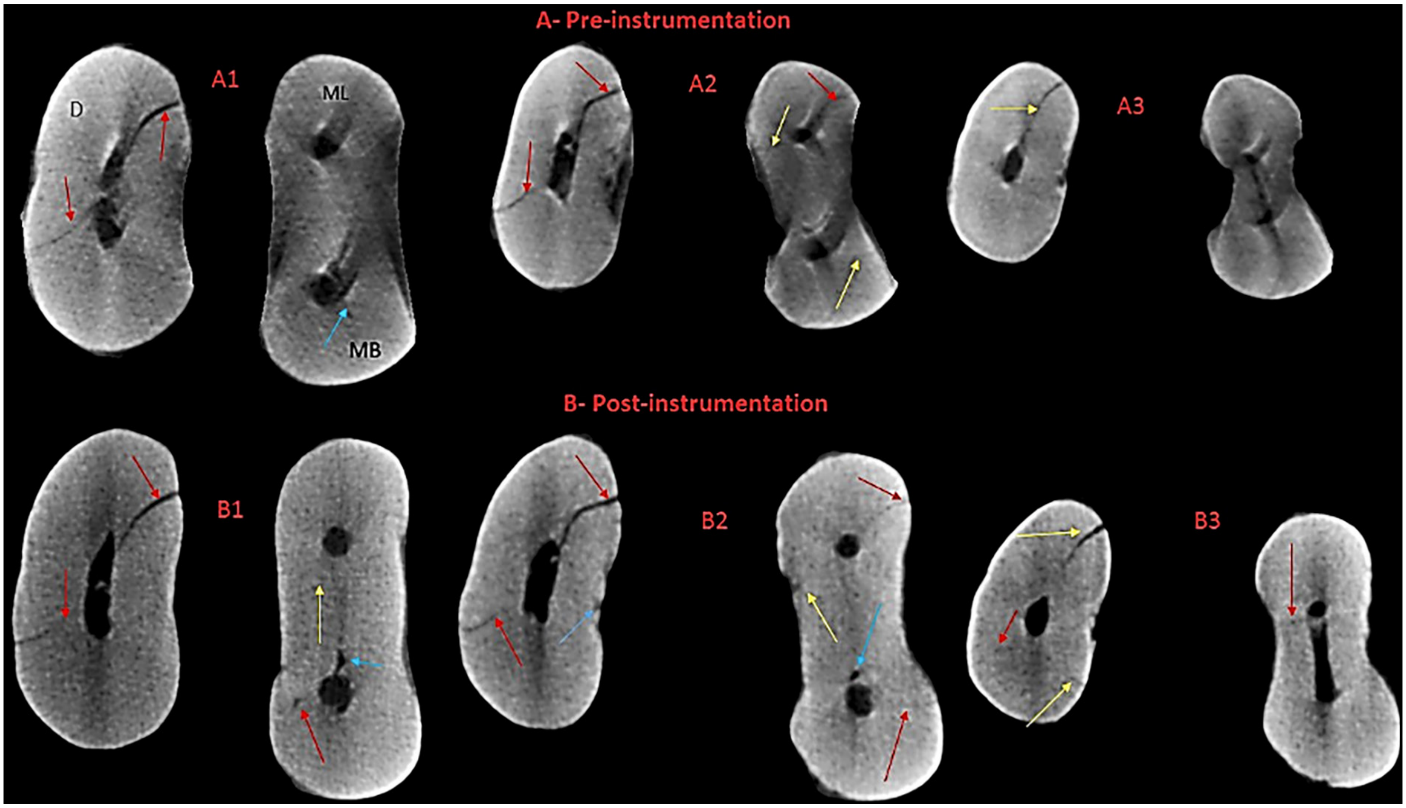

Figure 7. A: Micro-CT images for group TRNG pre-instrumentation showing microcracks at all levels: coronal (A1), middle (A2), apical (A3) as indicated by arrows (red: complete crack, blue: incomplete crack, yellow: craze line). B: Micro-CT images post-instrumentation showing microcrack at all levels: coronal (B1), middle (B2), apical (B3) as indicated by arrows (red: complete crack, blue: incomplete crack, yellow: craze line)

distal root. This might be attributed to the working length determination in this study, which was 1 mm short of the apical foramen.

Furthermore, more dentinal defects were present at the middle and coronal thirds for all groups, especially in the mesiobuccal root, because of the tortuous path, and an increase in the canal curvature increases the stress in the NiTi files (3). According to the results of this study in the distal root, the MTRN group showed a higher number of microcracks than MWOG at the coronal third. This result was attributed to increased taper for TRN prime, which was at D16=0.8 and D16=0.3 for WOG primary.

In this study, all roots of MFM were included without crown separation, and the samples were dried before micro-CT analysis was performed to allow visualisation of possible unnoticed microcracks (17). All samples collected for this study were stored in distilled water until the time of use to prevent post-mortem changes in dentinal structures (18).

Cone-beam computed tomography allows an improved precise procedure for measuring root canal curvature and working length. The non-destructive, high-resolution micro-CT technology ensures better visualisation of pre-existing dentinal defects at post-instrumentation stages (16).

From the result of the study, less incidence of newly formed microcracks was found for group WOGG, especially at the apical third (0.00%), followed by the middle third (2.04%). While no other studies assess the effect of WOGG and WOG primary on microcrack formation, the present result may indicate that alternating offset parallelogram cross-section and reciprocating motion resulted in less dentinal damage than continuous rotation motion (19). There was a high level of newly formed microcracks in group MWOG, especially in the middle third (20.41%). This result contrasts a previous study, which found less crack formation occurred with WOG (20). This discrepancy may be due to the previously mentioned study being conducted on single-rooted teeth (20); hence, there would have been less contact between the instrument and root surface, resulting in minimal stress and less crack formation.

Regarding the microcrack propagation among the study groups, the group TRNG, where the rotation glide path was performed using TRNG, showed less crack propagation. In agreement with a previous study, the appearance of the least propagated cracks in the fourth group could be attributed to the increased rotational speed, which is related to increased cutting efficiency and lesser crack formation and propagation. At the same time, the progressive taper and the slenderised pattern of TRNG might have caused relatively less apical crack propagation (21). Meanwhile, in contrast to this result, a high incidence of crack propagation with the TRN system was reported in a previous study in which 3D CAD model teeth with finite element analysis (FEA) were used (22). Moreover, the highest number of propagated microcracks was identified in group MWOG, especially at the coronal thirds. Haridas et al. (23) explained that the parallelogram cross-section of WOG files with two alternating 85° cutting edges and an off-centred cross-section means that the file contacts the root dentinal wall with only one cutting edge, which might increase the contact of the instrument with the dentinal wall, thus promoting the formation of dentinal defects. Additionally, the SS K-file's stiffness, combined with the file's aggressive tip in preparing the glide path, presents a great risk of affecting the canal geometry and causing crack propagation (24).

The engine-driven glide path (rotary TRNG and reciprocal WOGG) demonstrated a better effect on reducing crack formation and propagation when compared to manual glide path establishment. This result may be because of the instruments' design, flexibility, and kinematics, which make them more able to preserve the canal anatomy and root wall dentine, causing fewer aberrations and defects (25).

Nonetheless, another potential contributor to microcrack formation in this study is the NaOCl concentration of 5.2 %. NaOCl concentration influences the microcrack formation by degradation of the organic matrix of the root dentine to decrease the micro-hardness, elastic modulus, and flexural strength of the dentine (26).

From a clinical point of view, this study mimicked a clinical scenario by using extracted MFM teeth. Clinicians need to know that using glide path preparation before canal shaping gives better results in reducing microcrack formation and propagation. Additionally, using TRNG for glide path preparation is more effective in reducing the formation and propagation of microcracks.

Besides its use of micro-CT scans to analyse microcracks, there are limitations associated with this *in-vitro* study. Firstly, the detection of dentinal defects is influenced by the isotropic resolution of the micro-CT scan, so microcracks thinner than 20 µm might not have been detected. Furthermore, reconstruction image artefacts may be confused with dentinal microcracks or overlap with an existing microcrack, impeding its detection (27). Secondly, this *in-vitro* study was conducted on extracted teeth without a periodontal ligament. Other limitations of this study include its small sample size, non-inclusion of patient age, and use of curved and narrow canals. Moreover, this study combined different glide path techniques with root canal shaping systems to know their effect on microcrack formation and propagation.

Further research is required to compare the effect of different glide path techniques before root canal shaping in MFM teeth on dentinal microcrack formation and propagation using the previous or different files.

CONCLUSION

In conclusion, results on using micro-CT to analyse the incidence of microcracks in this study indicated that microcrack formation or propagation occurred regardless of the application of different types of glide path techniques (manual, rotary, and reciprocal).

Disclosures

Ethics Committee Approval: The study was approved by the College of Dentistry, University of Sulaimani Ethics Committee (no: 70/21, date: 09/11/2021).

Authorship Contributions: Concept – R.M.T.; Design – R.M.T.; Supervision – R.M.T.; Funding – S.F.J.; Materials – S.F.J.; Data collection and/or processing – S.F.J.; Data analysis and/or interpretation – S.F.J.; Literature search – S.F.J.; Writing – S.F.J.; Critical review – R.M.T.

Conflict of Interest: All authors declared no conflict of interest.

Use of AI for Writing Assistance: Not declared.

Financial Disclosure: The authors declared that this study received no financial support.

Peer-review: Externally peer-reviewed.

REFERENCES

1. Anous WH, Al-Ashry S, Ali MM, Kataia MM. Effect of different kinematic cutting motion in multiple versus single-file concept on dentinal crack formation: an *in vitro* study. J Int Oral Health 2020; 12(7):30–40. [CrossRef]
2. Shori DD, Shenoi PR, Baig AR, Kubde R, Makade C, Pandey S. Stereomicroscopic evaluation of dentinal defects induced by new rotary system: "ProTaper NEXT". J Conserve Dent 2015; 18(3):210–3. [CrossRef]
3. Kim HC, Lee MH, Yum J, Versluis A, Lee CJ, Kim BM. Potential relationship between design of nickel-titanium rotary instruments and vertical root fracture. J Endod 2010; 36(7):1195–9. [CrossRef]
4. Seirawan MY, Seirawan MK, Doumani M. Comparative evaluation of potential dentinal microcracks related to instrumentation alongside bypassed broken instruments: an *in vitro* study. J Contemp Dent Pract 2022; 23(1):14–21. [CrossRef]
5. de Oliveira BP, Câmara AC, Duarte DA, Heck RJ, Antonino ACD, Aguiar CM. Micro-computed tomographic analysis of apical microcracks before and after root canal preparation by hand, rotary, and reciprocating instruments at different working lengths. J Endod 2017; 43(7):1143–7. [CrossRef]
6. Xu X, Eng M, Zheng Y, Eng D. Comparative study of torsional and bending properties for six models of nickel-titanium root canal instruments with different cross-sections. J Endod 2006; 32(4):372–5. [CrossRef]
7. Ustun Y, Aslan T, Sagsen B, Kesim B. The effects of different nickel-titanium instruments on dentinal microcrack formations during root canal preparation. Eur J Dent 2015; 9(1):41–6. [CrossRef]
8. Unno H, Ebihara A, Hirano K, Kasuga Y, Omori S, Nakatsukasa T, et al. Mechanical properties and root canal shaping ability of a nickel-titanium rotary system for minimally invasive endodontic treatment: a comparative *in vitro* study. Materials (Basel) 2022; 15(22):792910. [CrossRef]
9. Kumar Katta P. Reciprocating files in endodontics. J Res Med Dent Sci 2022; 10(10):15–22.
10. van der Vyver PJ, Vorster M, Peters OA. Minimally invasive endodontics using a new single-file rotary system. Int Dent - African Ed 2019; 9(4):6–20.
11. Chandrasekhar M, Reddy SNL, Moosani GK, Upendranatha R, Nikhita K, Kumar MP. Influence of rotary and reciprocating glide path techniques on the incidence of dentinal crack formation– an *in vitro* study. Int J Contemp Med Res 2016; 3(7):2075–8.
12. Ajina M, Billis G, Chong BS. The effect of glide path preparation on root canal shaping procedures and outcomes. Eur Endod J 2022; 7(2):92–105. [CrossRef]
13. Schneider SW. A comparison of canal preparations in straight and curved root canals. Oral Surg Oral Med Oral Pathol 1971; 32(2):271–5. [CrossRef]
14. Zarean P, Özcan M, Zarean P, Haghani SO, Jahromi MZ, Al-Haj Husain N, et al. Micro-computed tomographic assessment of microcrack formation before and after instrumentation of curved root canals with Neoniti rotary files. Materials (Basel) 2022; 15(9):3002. [CrossRef]
15. Martins JCLGD, Oliveira BP, Duarte DA, Antonino ACD, Aguiar CM, Câmara AC. Micro-computed tomographic assessment of dentinal microcrack formation in straight and curved root canals in extracted teeth prepared with hand, rotary and reciprocating instruments. Int Endod J 2021; 54(8):1362–8. [CrossRef]
16. Arumugam S, Yew HZ, Baharin SA, Qamaruz Zaman J, Muchtar A, Kanagasingam S. Micro-computed tomography evaluation of dentinal microcracks following canal preparation with thermomechanically heat-treated engine-driven files. Aust Endod J 2021; 47(3):520–30. [CrossRef]
17. Rödig T, Müller C, Hoch M, Haupt F, Schulz X, Wiegand A, Rizk M. Moisture content of root canal dentine affects detection of microcracks using micro-computed tomography. Int Endod J 2018; 51(3):357–63. [CrossRef]
18. Aydın B, Pamir T, Baltaci A, Orman MN, Turk T. Effect of storage solutions on microhardness of crown enamel and dentin. Eur J Dent 2015; 9(2):262–6. [CrossRef]
19. Shashidhar C, Rao D, Naik S, Shashidhar J. Rotary versus reciprocating file system: an *in vitro* stereomicroscopic evaluation of radicular dentinal cracks formation at various root levels. Int J Sci Res 2019; 8:71–4.
20. Rahman H, Chandra A, Khangwal M, Goel A, Shakya VK. Stereomicroscopic evaluation of microcrack formation in dentin by ProTaper Next, Revo S, and WaveOne Gold file system. Contemp Clin Dent 2021; 12(4):439–43.
21. Kumar GV, Shahina P, Kumar AM, Kumar LL, Kishore BK, Anukrati S. Comparative evaluation of dentinal cracks formation after root canal preparation using three different rotary file systems- a stereomicroscopic *in vitro* study. Natl Res Denticon 2023; 12:1–10.
22. Hassanain Z. The influence of peri-cervical dentin conservation on the propagation of cracks in mandibular molars. Marq Univ J 2023; 4:5534.
23. Haridas K, Hariharan M, Singh P, Varughese A, Ravi AB, Venugopal K. Comparative evaluation of microcrack formation in different kinematics using rotary and reciprocating file systems: an *in vitro* study. J Contemp Dent Pract 2020; 21(12):1389–92. [CrossRef]
24. Sharma S, Dhillon JS, Singh H, Kaur M. Establishing glide path-the instrumentation secret. Int J Curr Res 2016; 8:37343–7.
25. van der Vyver PJ, Vorster M, Paleker F, De Wet FA. Glide path preparation in endodontics: case report and a literature review of available materials and techniques. S Afr Dent J 2019; 74:129–36. [CrossRef]
26. Abou Almakarem HM, Genena SMH, Abd El Motie MA, Zaazou AM, Mokhless A. incidence of dentinal defect after root canal preparation using Hyflix EDM, and MPRO files (*in vitro* study). Alex Dent J 2020; 46(1):123–8.
27. De-Deus G, Cavalcante DM, Belladonna FG, Carvalhal J, Souza EM, Lopes RT, et al. Root dentinal microcracks: a post-extraction experimental phenomenon. Int Endod J 2019; 52(6):857–65. [CrossRef]